Dystrophin is a microtubule-associated protein

Kurt W. Prins,[1] Jill L. Humston,[2] Amisha Mehta,[3] Victoria Tate,[3] Evelyn Ralston,[3] and James M. Ervasti[1,2]

[1]Department of Biochemistry, Molecular Biology, and Biophysics, University of Minnesota, Minneapolis, MN 55455
[2]Molecular and Cellular Pharmacology Training Program, University of Wisconsin, Madison, WI 53706
[3]Light Imaging Section, Office of Science and Technology, National Institute of Arthritis and Musculoskeletal and Skin Diseases, National Institutes of Health, Bethesda, MD 20892

Cytolinkers are giant proteins that can stabilize cells by linking actin filaments, intermediate filaments, and microtubules (MTs) to transmembrane complexes. Dystrophin is functionally similar to cytolinkers, as it links the multiple components of the cellular cytoskeleton to the transmembrane dystroglycan complex. Although no direct link between dystrophin and MTs has been documented, costamere-associated MTs are disrupted when dystrophin is absent. Using tissue-based cosedimentation assays on mice expressing endogenous dystrophin or truncated transgene products, we find that constructs harboring spectrinlike repeat 24 through the first third of the WW domain cosediment with MTs. Purified Dp260, a truncated isoform of dystrophin, bound MTs with a K_d of 0.66 µM, a stoichiometry of 1 Dp260/1.4 tubulin heterodimer at saturation, and stabilizes MTs from cold-induced depolymerization. Finally, α- and β-tubulin expression is increased ∼2.5-fold in *mdx* skeletal muscle without altering the tubulin–MT equilibrium. Collectively, these data suggest dystrophin directly organizes and/or stabilizes costameric MTs and classifies dystrophin as a cytolinker in skeletal muscle.

Introduction

The plakins are a class of giant cytolinker proteins that can link transmembrane protein complexes to the actin, intermediate filament, and microtubule (MT) cytoskeletons in various combinations (Fuchs and Karakesisoglou, 2001). Plakins can bind actin filaments via tandem calponin homology (CH) domains, intermediate filaments via plakin repeat domains, and MTs through either a Gas2-related domain or a glycine/serine/arginine domain (for review see Leung et al., 2002). The ability to cross-link multiple components of the cellular cytoskeleton allows cytolinkers to stabilize cells from mechanically induced damage. Mouse knockout studies exemplify the stabilizing effects of cytolinkers, as loss of the cytolinker plectin resulted in skin blistering and a form of muscular dystrophy (Andra et al., 1997), and ablation of BPAG-1, another cytolinker, caused skin blistering upon mechanical stimulation (Guo et al., 1995).

Dystrophin, the protein absent in patients with Duchenne muscular dystrophy (Hoffman et al., 1987), shows structural and functional similarities to cytolinkers, which suggests the hypothesis that dystrophin performs a cytolinker role in muscle. Dystrophin's large molecular mass of 427 kD, spectrinlike repeats, and ability to bind actin filaments via a tandem CH domain (Way et al., 1992) highlight three similarities with cytolinkers. Although dystrophin lacks a plakin repeat domain, dystrophin–intermediate filament interactions have been documented (Stone et al., 2005; Bhosle et al., 2006). Thus, the ability to link the actin and intermediate filament cytoskeletons to the transmembrane dystroglycan complex (Suzuki et al., 1992) illustrates how dystrophin functions similarly to other cytolinkers. Finally, the muscle membrane fragility associated with the loss of dystrophin (Petrof et al., 1993) parallels the structural deficiencies observed in other cytolinker-deficient tissues, further demonstrating a close relationship between dystrophin and other cytolinkers. Collectively, these data support the hypothesis that dystrophin may function as a cytolinker in skeletal muscle.

Although dystrophin exhibits many characteristics of a cytolinker, a direct dystrophin–MT interaction has not been documented. Dystrophin lacks either a Gas2-related or a glycine/serine/arginine domain, but recent studies indicated that dystrophin at least indirectly influences MT organization or stability (Percival et al., 2007; Ayalon et al., 2008). For instance, the dystrophin-deficient *mdx* mouse exhibited MT disorganization in skeletal muscle with the costameric MTs most severely affected (Percival et al., 2007). Dystrophin's enrichment at costameres

Correspondence to James M. Ervasti: jervasti@umn.edu

Abbreviations used in this paper: CH, calponin homology; MAP, MT-associated protein; MOM, mouse on mouse; MT, microtubule; wt, wild type.

The Rockefeller University Press $30.00
J. Cell Biol. Vol. 186 No. 3 363–369
www.jcb.org/cgi/doi/10.1083/jcb.200905048

and the restoration of costameric MT organization through virally mediated expression of a microdystrophin (Percival et al., 2007) indicates that dystrophin is necessary for proper costameric MT organization in skeletal muscle. Moreover, acute knockdown of ankyrin-B, a protein necessary for delivery of dystrophin to the sarcolemma and neuromuscular junction, caused the loss of costameric MTs and aberrant MT organization in a subset of MTs underlying the neuromuscular junction (Ayalon et al., 2008).

In this study, we investigated the hypothesis that dystrophin directly interacts with costameric MTs. We confirmed that costameric MTs were disrupted in dystrophin-deficient skeletal muscle and showed endogenous dystrophin cosedimented with MTs in tissue homogenates. Using purified proteins, we found that the carboxyl-terminal two thirds of dystrophin bound MTs with a K_d of 0.66 µM and stabilized MTs from cold-induced depolymerization. Finally, we documented a 2.5-fold increased expression of α- and β-tubulin without alteration in the tubulin–MT equilibrium in *mdx* skeletal muscle. These results demonstrate that dystrophin is a MT-associated protein (MAP) that stabilizes costameric MTs and functions as a costameric cytolinker in skeletal muscle.

Results and discussion

To determine whether dystrophin and MTs localize to similar structures in skeletal muscle, we conducted immunofluorescence analysis on teased extensor digitorum longus muscle fibers colabeled with antidystrophin and anti–α-tubulin antibodies (Fig. 1, A and B). Dystrophin forms a subsarcolemmal network with transverse components along the I bands and the M line and with longitudinal components (Williams and Bloch, 1999), whereas MTs form a subsarcolemmal lattice, which in fast fibers, has transverse and longitudinal components plus an accumulation of MTs around myonuclei (Ralston et al., 1999). We found that the transverse MTs (Fig. 1 A, arrowheads) weave their course along the I band dystrophin staining for long distances. MTs were also associated with longitudinal lines of dystrophin (Fig. 1 A, arrows). These data identify domains of the subsarcolemmal cytoskeleton where dystrophin and MTs may interact either directly or indirectly. Next, we examined MT organization in mouse models lacking dystrophin (*mdx*), dystrophin's autosomal homologue utrophin ($utrn^{-/-}$), or both dystrophin and utrophin ($mdx/utrn^{-/-}$). Consistent with previous results (Percival et al., 2007), loss of dystrophin resulted in MT disorganization with the costameric MTs appearing to be most severely affected (Fig. 1 C) when compared with wild type (wt; Fig. 1 C). Ablation of utrophin had no effect on MT organization (Fig. 1 C), which is likely a result of its very low expression (Rybakova et al., 2002) and restriction to the neuromuscular junction (Ohlendieck et al., 1991). Finally, $mdx/utrn^{-/-}$ skeletal muscle exhibited MT disorganization comparable with that of *mdx* (Fig. 1 C). MT organization in 24-d-old prenecrotic *mdx* skeletal muscle fibers was also disorganized, whereas age-matched wt mice displayed a MT lattice nearly identical to mature wt mice (Fig. 1 D). Collectively, these results confirm a role for dystrophin in the stabilization and proper organization of costameric MTs independent of muscle necrosis and regeneration.

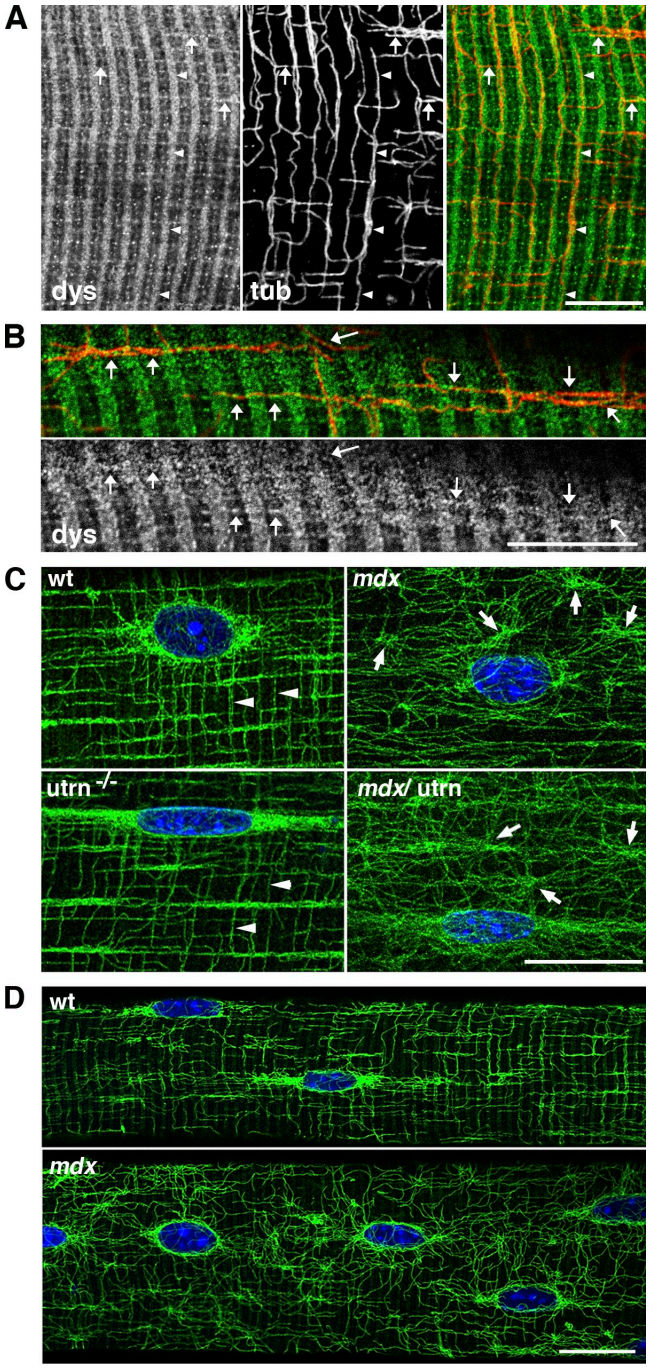

Figure 1. **Dystrophin guides MTs at the surface of the muscle fibers and is necessary for proper MT organization.** (A) Isolated muscle fibers from the extensor digitorum longus of 7-wk-old wt mice were costained for dystrophin (left) and α-tubulin (middle). The right panel shows that MTs (red) follow dystrophin (green) bands for long distances both transversely (arrowheads) and longitudinally (arrows). (B) At a higher magnification, dystrophin staining is granular; MTs are studded with dystrophin "dots." Arrows indicate longitudinal MTs that follow dystrophin. (C) Muscle fibers from the extensor digitorum longus of 7-wk-old wt, *mdx*, $utrn^{-/-}$, and $mdx/utrn^{-/-}$ mice were stained with DM1A anti–α-tubulin and Hoechst dye. Both wt and $utrn^{-/-}$ fibers show the lattice of transverse and longitudinal MTs characteristic of fast fibers (arrowheads). In *mdx* and $mdx/utrn^{-/-}$ fibers, the regularity of the lattice is lost, and mostly oblique MTs originate from cytoplasmic nucleation points (arrows). (D) Peripherally nucleated prenecrotic muscle fibers from 24-d-old *mdx* mice also displayed MT disorganization, indicating that MT derangement occurred before muscle cell necrosis and regeneration. Bars: (A and B) 10 µm; (C and D) 20 µm.

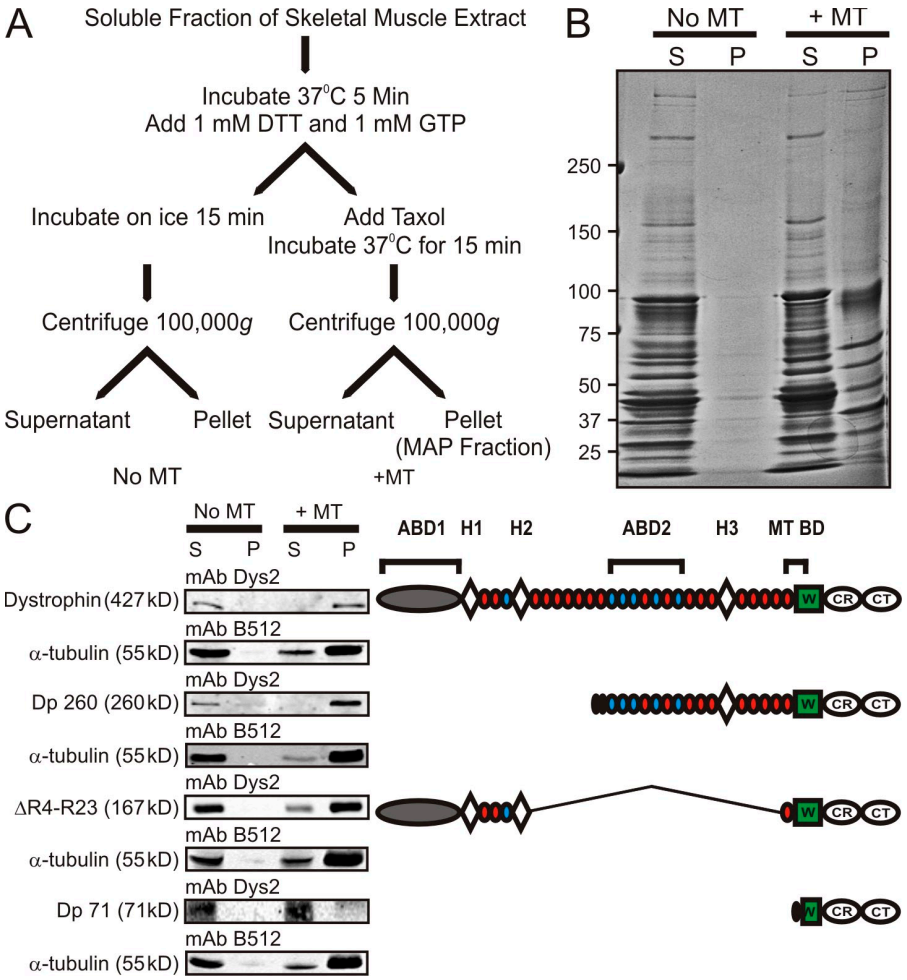

Figure 2. **Dystrophin cosediments with MTs in skeletal muscle extracts.** (A) Flowchart of tissue MT cosedimentation assay. (B) Coomassie blue–stained SDS-PAGE showing supernatant (S) and pellet (P) fractions in conditions that favored MT depolymerization or polymerization. The pellet fraction in the presence of MTs represents the MAP fraction of skeletal muscle. The molecular mass standards (given in kilodaltons) are indicated on the left. (C, left) Western blot analysis of tissue cosedimentation assay from skeletal muscle extracts of wt mice expressing dystrophin or *mdx* mice transgenically expressing Dp260, ΔR4-R23, and Dp71. (right) Diagrammatic representation of constructs analyzed in tissue cosedimentation. ABD, actin-binding domain; H, hinge region; W, WW domain; CR, cysteine-rich domain; CT, carboxy-terminal domain; MT BD, MT-binding domain.

Next, we performed a tissue-based MT cosedimentation assay (Fig. 2 A) to determine whether dystrophin cosedimented with MTs. Under conditions that induced MT depolymerization, virtually no muscle protein pelleted (Fig. 2 B). However, numerous proteins pelleted under MT-stabilizing conditions, and this fraction of proteins represents MTs and the MAPs of skeletal muscle (Fig. 2 B). We Western blotted each fraction obtained from the tissue cosedimentation assay performed on wt mice expressing full-length dystrophin or transgenic *mdx* mice expressing Dp260, microdystrophin (ΔR4-23), or Dp71 (Fig. 2 C, right). Full-length dystrophin, Dp260, and ΔR4-23 all pelleted with MTs, whereas Dp 71 did not (Fig. 2 C, left). By comparing the dystrophin domains present or absent in each construct (Fig. 2 C, right) along with each construct's ability to cosediment with MTs, we suggest that spectrinlike repeat 24 through the first third of the WW domain encodes a novel MT-binding domain.

To test for a direct interaction between dystrophin and MTs, we performed MT cosedimentation using two purified recombinant dystrophin constructs and purified tubulin. The two recombinant constructs used were Dp260, which encodes from spectrinlike repeat 10 through the carboxy terminus of dystrophin, including the proposed MT-binding domain, and $DysN_{Term}$-R_{10} (Rybakova et al., 2006), which encodes the amino-terminal, tandem CH actin-binding domain and spectrinlike repeats 1–10 of the middle rod domain absent from Dp260. A small amount of Dp260 pelleted in the absence of MTs, but substantially more Dp260 shifted to the pellet fraction when MTs were present (Fig. 3 A). After subtracting self-pelleting Dp260, Dp260 displayed a concentration-dependent and saturable cosedimentation with a Dp260/α-β tubulin heterodimer stoichiometry of 1:1.4 and a K_d of 0.66 μM (Fig. 3 C). As predicted, $DysN_{Term}$-R_{10} did not cosediment with MTs up to concentrations approaching 10 μM (Fig. 3, B and C). Next, we assessed how the presence of 1 μM Dp260 affected the tubulin–MT equilibrium in vitro. Dp260 had no significant effect on the fraction of tubulin in the MT fraction when incubated at room temperature (67.3 ± 0.72% vs. 68.6 ± 1.3%). However, the presence of Dp260 significantly increased the fraction of tubulin retained in the MT pellet (33.6 ± 2.9% vs. 42.2 ± 2.0%) when MTs were induced to depolymerize by incubating at 4°C. (Fig. 3, D and E). Collectively, these results demonstrate that dystrophin directly binds and stabilizes MTs from cold-induced depolymerization.

Because misregulation of other MAPs can alter tubulin expression and MT stability (Harada et al., 1994; Takahashi et al., 2003), we investigated how the loss of dystrophin affects the regulation of tubulin expression and the tubulin–MT equilibrium in skeletal muscle fibers. Tubulin levels in wt and *mdx* skeletal muscle extracts were examined by quantitative Western blot analysis. With mAb B512, we observed no difference

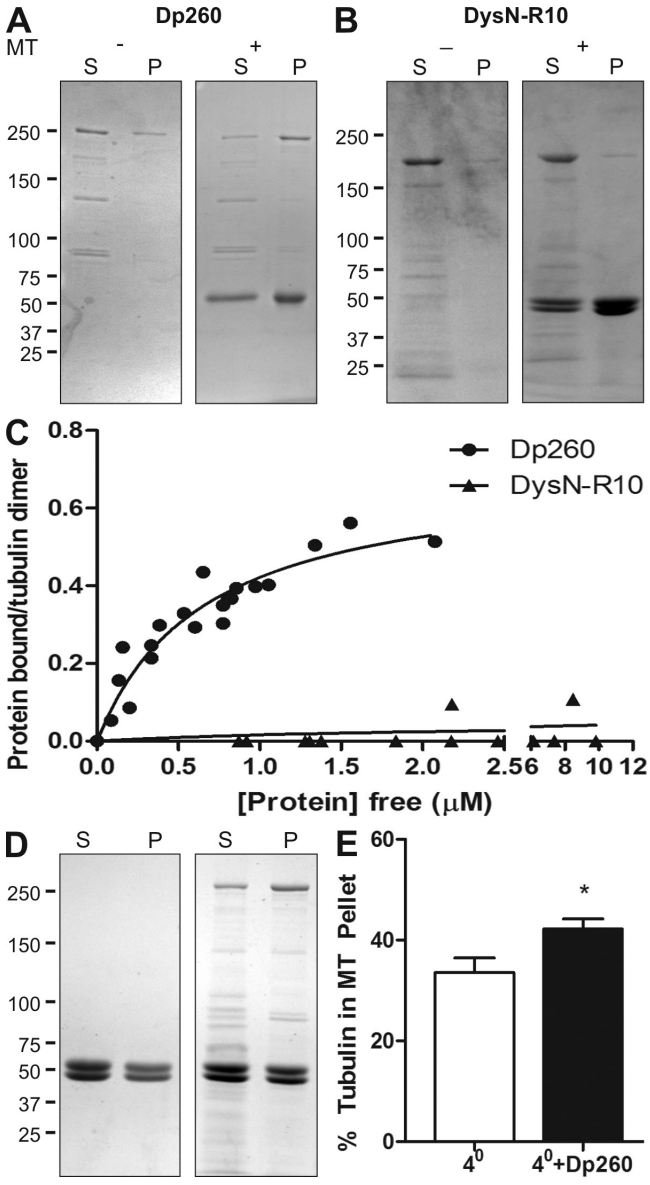

Figure 3. **Dp260 binds and stabilizes MTs in vitro.** (A) Coomassie blue–stained SDS-PAGE showing the supernatant (S) and pellet (P) fractions of purified Dp260 in the presence and absence of MTs. Dp260 shifted to the pellet fraction when MTs were present, indicating that Dp260 binds MTs. (B) Coomassie blue–stained SDS-PAGE showing the supernatant and pellet fractions of DysN-R_{10} in the presence and absence of MTs. The presence of MTs did not cause a shift of DysN-R_{10} into the pellet fraction, indicating that DysN-R_{10} does not bind MTs. (C) Concentration-dependent binding of Dp260 to taxol-stabilized MTs (2 μM tubulin) from three independent experiments. DysN-R_{10} did not show significant MT-binding activity. (D) Coomassie blue–stained SDS-PAGE of the supernatant and pellet fractions of MTs induced to depolymerize by incubating at 4°C in the presence or absence of 1 μM Dp260. (E) Quantification of tubulin in the MT fraction when induced to depolymerize by incubating at 4°C ($n = 6$). The presence of 1 μM Dp260 significantly (*t* test; *, $P \leq 0.05$) increased the amount of tubulin in the MT fraction, indicating that Dp260 stabilizes MTs. Error bars represent mean ± SEM. (A, B, and D) Molecular mass standards (given in kilodaltons) are indicated on the left.

in α-tubulin expression between wt and *mdx* skeletal muscle extracts (Fig. 4, A and B), which was consistent with what we (Prins et al., 2008) and others (Barton et al., 2002) reported previously. However, mAb DM1A showed an ∼2.5-fold increase in α-tubulin expression in *mdx* skeletal muscle (Fig. 4, A and B). Because levels of α- and β-tubulin are coregulated (Gonzalez-Garay and Cabral, 1995), we investigated β-tubulin levels to determine whether α-tubulin is up-regulated in *mdx* skeletal muscle. β-Tubulin expression was elevated 2.5-fold in *mdx* skeletal muscle (Fig. 4, A and B), suggesting that expression of both α- and β-tubulin is increased in *mdx* skeletal muscle. Thus, we conclude that mAb DM1A is able to recognize a population of α-tubulin not detected by mAb B512. To examine MT stability in *mdx* skeletal muscle, we analyzed levels of tyrosinated α-tubulin, a marker of dynamic MTs (Gundersen et al., 1984, 1987), and acetylated α-tubulin, a marker of long-lived MTs (Bulinski and Gundersen, 1991). The levels of tyrosinated α-tubulin were increased ∼2.5-fold in *mdx* extracts (Fig. 4, A and B), whereas the levels of acetylated α-tubulin were not (Fig. 4, A and B). The loss of dystrophin's MT-stabilizing ability may explain why acetylated α-tubulin was not more abundant in *mdx* skeletal muscle extracts, but alterations in the tubulin–MT equilibrium could also explain the lack of more stable MTs. Therefore, we examined the tubulin–MT equilibrium in wt and *mdx* skeletal muscles and found that the loss of dystrophin did not affect the equilibrium (Fig. 4, C and D). Collectively, these results show that tubulins are misregulated in dystrophin-deficient skeletal muscle without affecting the tubulin–MT equilibrium. The loss of dystrophin's MT-stabilizing ability likely explains why there are not more stabilized MTs even in the presence of more tubulin dimer in dystrophin-deficient skeletal muscle.

An indirect link between dystrophin and MTs mediated by ankyrin-B was recently shown to be important for proper trafficking of dystrophin and β-dystroglycan to the sarcolemma (Ayalon et al., 2008). However, costameric MTs are disorganized in *mdx* skeletal muscle even in the presence of properly localized ankyrin-B (Ayalon et al., 2008). Because the MT- and ankyrin-B–binding domains of dystrophin do not overlap (Fig. 5), our results and previous results suggest that dystrophin interacts with MTs in vivo through two distinct mechanisms. We propose that ankyrin-B delivers dystrophin to the sarcolemma dependent on MTs and that dystrophin and ankyrin-B collaborate to stabilize and organize MTs in skeletal muscle.

As with other cytolinkers, the ability to bind multiple components of the filamentous cytoskeleton likely allows dystrophin to protect the sarcolemma from mechanically induced damage. One highly truncated microdystrophin construct (ΔR4-23) is very effective in restoring function in the dystrophin-deficient *mdx* mouse (Harper et al., 2002). Interestingly, the ΔR4-23 microdystrophin contains all sequences required for interaction with the three cytoskeletal filament systems: the amino-terminal tandem CH domain, which binds actin (Way et al., 1992) and cytokeratin filaments (Stone et al., 2005), the spectrinlike repeat 3 and the cysteine-rich regions, which are necessary for synemin intermediate filament binding (Bhosle et al., 2006), and the MT-binding domain. In contrast, Dp260 lacks the cytokeratin filament–binding domain and portions of the synemin- and actin-binding domains, which likely alters the binding affinities to both actin and synemin filaments and may explain why transgenic overexpression of Dp260 only partially alleviates the *mdx*

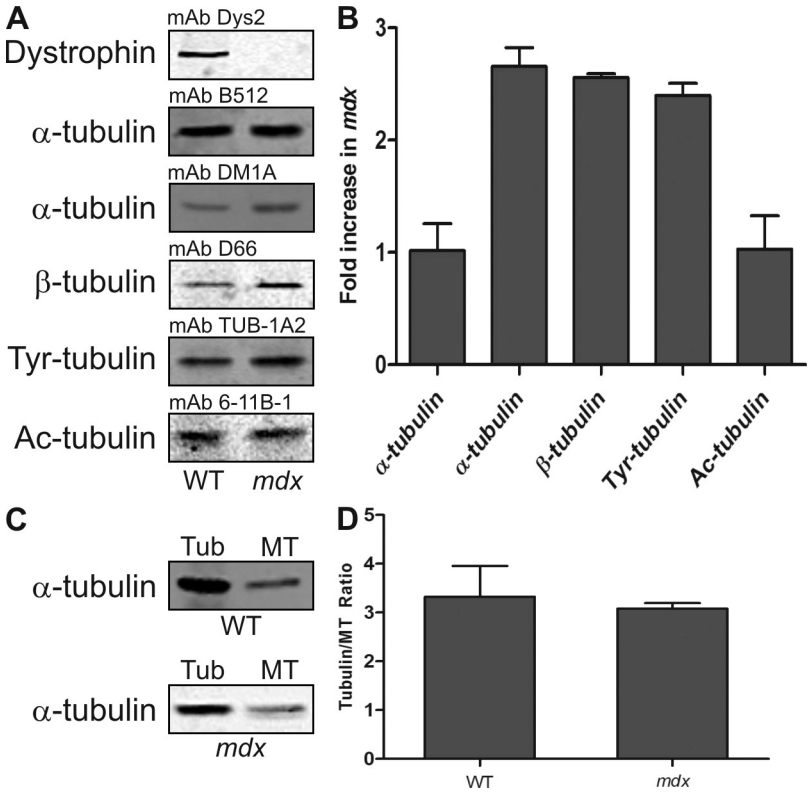

Figure 4. ***Mdx* mice exhibit tubulin misregulation in the absence of an altered tubulin–MT equilibrium.** (A) Representative Western blots of tubulin levels in skeletal muscle extracts from wt and *mdx* mice. (B) Quantification of tubulin levels from three wt and three *mdx* extracts. (C) Representative Western blots of tubulin (tub) and MT fractions of skeletal muscle extracts from wt and *mdx* mice using mAb DM1A. (D) Quantification of tubulin–MT equilibrium from five wt and four *mdx* tibialis anterior muscles. Loss of dystrophin does not affect the tubulin–MT equilibrium. Error bars represent mean ± SEM.

phenotype (Warner et al., 2002). Because Dp116 harbors only the MT-binding domain and one of two synemin-binding sequences, an inability to bind cytokeratin filaments and actin filaments likely explains why transgenic overexpression of Dp116 fails to rescue the *mdx* phenotype (Judge et al., 2006). Finally, the mild muscle phenotypes of γ_{cyto}-actin (Sonnemann et al., 2006) or keratin 19 knockout mice (Stone et al., 2007) may be explained by dystrophin's linkage with the remaining components of the cortical cytoskeleton. Collectively, these results support the hypothesis that dystrophin must bind all three components of the cellular cytoskeleton to function properly in skeletal muscle.

Although the dystrophin–MT interaction fits well with the structural/organization functions previously ascribed to dystrophin, the importance of MTs in trafficking of proteins, vesicles, organelles, and mRNAs (for review see Hirokawa and Noda, 2008; Gennerich and Vale, 2009) also suggests how MT disruption in *mdx* skeletal muscle could contribute to the dystrophic pathophysiology. For example, disorganized MTs are also associated with Golgi mislocalization (Percival et al., 2007), which in combination, would likely lead to impaired trafficking of membrane-bound proteins and may explain the decreased levels of β-dystroglycan and the sarcoglycans at the sarcolemma of *mdx* skeletal muscle (Ohlendieck and Campbell, 1991). Because no MT knockout mouse has been generated, the exact function of MTs in skeletal muscle remains unknown. However, the importance of MTs in skeletal muscle biology is illustrated by the muscle weakness and increased levels of serum creatine kinase associated with colchicine toxicity in human patients (Boomershine, 2002; Caglar et al., 2003; Wilbur and Makowsky, 2004; Altman et al., 2007). Therefore, it is possible that derangement of the MT cytoskeleton contributes to some of the phenotypes associated with dystrophin deficiency.

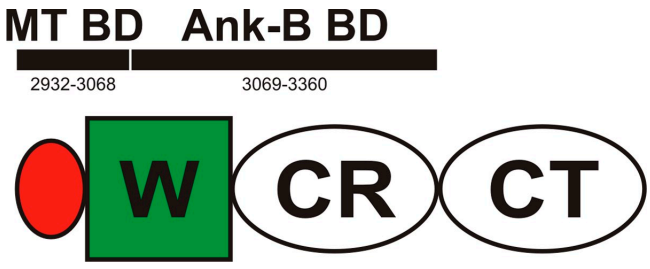

Figure 5. **Diagrammatic representation of MT- and ankyrin-B–binding domains of dystrophin.** Numbers indicate amino acids of full-length dystrophin. H, hinge region; W, WW domain; CR, cysteine-rich domain; CT, carboxy-terminal domain; MT BD, MT-binding domain; Ank-B BD, ankyrin-B–binding domain.

Materials and methods

Mice

Control C57BL/6 and *mdx* mice were initially obtained from The Jackson Laboratory. The *utrn*$^{-/-}$ and *mdx*/*utrn*$^{-/-}$ mice were provided by D. Lowe (University of Minnesota, Minneapolis, MN). *Mdx* mice transgenically expressing Dp260 and ΔR4-R23 were provided by J. Chamberlain (University of Washington, Seattle, WA), and the Dp71 line was provided by J. Rafael-Fortney (Ohio State University, Columbus, OH). All animals were housed and treated following guidelines set by the University of Minnesota Institutional Animal Care and Use Committee.

Antibodies

The mAbs to α-tubulin (B512), β-tubulin (D66), tyrosinated tubulin (TUB 1-A2), and acetylated tubulin (6-11B-1) were purchased from Sigma-Aldrich. The mAb to α-tubulin (DM1A) was purchased from Abcam. The mAb to dystrophin (Dys2) was purchased from Novacastra. The polyclonal antibody to dystrophin (Rb2) was described previously (Rybakova et al., 1996). Infrared dye–conjugated anti–mouse secondary antibodies were purchased from LI-COR Biosciences.

Immunofluorescence analysis

To analyze the MT lattice in dystrophic animal models, hindlegs of wt (3 and 8 wk), *mdx* (3, 5, and 8 wk), *utrn*$^{-/-}$ (8–10 wk), and *mdx:utrn*$^{-/-}$ (3, 5, and 8 wk) mice were skinned, cut as close as possible to the body, and fixed at room temperature for 2 h with 4% para-formaldehyde in phosphate buffer. They were stored in phosphate buffer until the extensor digitorum longus muscle was dissected and separated with fine forceps into mostly single fibers. These were transferred to a 24-well tissue culture plate and incubated with mouse on mouse (MOM)–blocking buffer (Vector Laboratories) for 2 h at room temperature. Blocking buffer and every subsequent buffer for incubation or washing contained 0.04% saponin for permeabilization and 0.05% sodium azide. Fibers were incubated overnight with mouse antitubulin (DM1A, 1:500; or B512, 1:4,000) in MOM diluent, washed three times for 20 min, and stained with 1:500 dilutions of Alexa Fluor 488 anti–mouse and Alexa Fluor 568 anti–rabbit secondary antibodies (Invitrogen) in MOM diluent for 2 h at room temperature. After three 20-min washes, one of which contained the nuclear stain Hoechst 33342 (Sigma-Aldrich) at 2 µg/ml, fibers were mounted onto a glass slide in a drop of Vectashield (Vector Laboratories). Confocal images were captured with a 63× NA 1.4 oil immersion lens on a TCS SP5 confocal microscope (Leica) in the Light Imaging Section of the National Institute of Arthritis and Musculoskeletal and Skin Diseases. Gain and laser power settings were adjusted to avoid saturation and use the whole linear range of fluorescence intensity. Unless specified, the parameters were adjusted for each new fiber imaged. The raw TIF images were transferred to a computer (Macintosh G5; Apple), opened in Photoshop (CS2; Adobe), assembled into montages, and adjusted for brightness when needed. The final illustrations give a faithful representation of the collected images.

Tissue MT cosedimentation assay

Tissue-based cosedimentation was performed as described previously (Hughes et al., 2008) with the following exception. The starting material was 200 mg of frozen skeletal muscle that was pulverized in a mortar and pestle cooled with liquid nitrogen then added to MT buffer (1% Triton X-100, 50 mM Hepes, 50 mM KCl, 1 mM $MgCl_2$, 1 mM EGTA, 0.75 mM benzamidine, 0.1 mM PMSF, 0.6 µg/ml pepstatin A, 0.5 µg/ml aprotinin, 0.5 µg/ml leupeptin, iodoacetamide, and E64). The extracts were incubated for 1 h at 4°C and centrifuged at 100,000 *g* for 40 min at 25°C. 1 mM of both GTP and DTT was added to the soluble fraction of the extract and incubated at 37°C for 5 min. The extract was split into two fractions, one that was incubated on ice for 15 min, and 20 µM taxol was added to the other and incubated at 37°C for 15 min. 300 µl of each fraction was layered onto a cushion buffer (MT buffer plus 40% sucrose) and centrifuged at 100,000 *g* for 30 min at 25°C. The supernatant was removed, and the pellet fraction was resuspended in a Laemmli sample buffer.

Protein purification

A cDNA-encoding Flag-tagged Dp260 (Warner et al., 2002) provided by J. Chamberlain was cloned into pFASTbac1 to generate a recombinant baculovirus expression vector using previously described methods (Rybakova et al., 2002). Dp260 and dystrophin N_{term}-R_{10} were expressed and purified using the baculovirus expression system and anti-Flag M2 affinity chromatography, respectively, as previously described (Rybakova et al., 2002), except the proteins were dialyzed into MT buffer without Triton X-100. Protein concentration was determined using A_{280} using Nanodrop software with an extinction coefficient of 272,495 M^{-1} cm^{-1} for Dp260 and 221,115 M^{-1} cm^{-1} for DysN-R_{10} as predicted by the Expert Protein Analysis System proteomics server (Swiss Institute of Bioinformatics).

MT cosedimentation analysis

MT cosedimentation assay was performed as described by the manufacturer's instructions (Cytoskeleton, Inc). In brief, increasing amounts of purified protein were added to preformed MTs then centrifuged at 100,000 *g* for 30 min. The amount of free and bound protein was determined densitometrically from Coomassie blue–stained gels of the supernatant and pelleted fractions using imaging system software (UVP). The fraction of protein pelleting in the absence of MTs was subtracted from each data point. The resultant data from three independent experiments were fitted to a hyperbolic binding equation using nonlinear regression analysis on Prism software (GraphPad Software, Inc.).

Cold-induced depolymerization assay

Tubulin was induced to polymerize as described by the manufacturer's instructions (Cytoskeleton, Inc.) and incubated with 1 µM Dp260. The reactions were incubated at 4°C for 30 min then centrifuged at 100,000 *g* for 30 min at 4°C. The supernatant and pellet fractions were prepared and quantified as described in the previous paragraph.

Western blot analysis and quantification

Western blot analysis and quantification from three wt and three *mdx* skeletal muscle extracts were performed as described previously (Prins et al., 2008). In brief, 25 µg of skeletal muscle extract was subjected to SDS-PAGE and transferred to nitrocellulose membranes, which were washed/blocked in a 5% milk solution in PBS for 1 h. The membranes were incubated overnight with primary antibody at room temperature. The primary antibodies and dilutions used were mAb Dys2 (1:50), mAb B512 (1:250), mAb DM1A (1:250; Sigma-Aldrich), mAb D66 (1:100), and mAb 6-11B-1 (1:100). Membranes were washed two times for 10 min in 5% milk solution at room temperature, incubated with infrared dye–conjugated secondary antibody (1:10,000) for 30 min at room temperature, and the membranes were washed in a 0.5% Tween solution in PBS two times for 10 min. Western blots were imaged and quantified with an infrared imaging system (Odyssey; LI-COR Biosciences). The Coomassie blue–stained posttransfer gel was analyzed densitometrically using UVP software and served as the loading control.

In vivo tubulin–MT equilibrium assay

The tibialis anterior was dissected, immediately placed in 1 ml of MT stabilization buffer (1% Triton X-100, 50% glycerol, 5% DMSO, 10 mM Na_2HPO_4, 0.5 mM EGTA, and 0.5 mM $MgSO_4$), and homogenized with 10 strokes in a homogenizer. The resulting homogenate was centrifuged at 100,000 *g* for 30 min at 25°C. The soluble portion (tubulin containing) was saved for analysis, whereas the pelleted portion (MT fraction) was resuspended in 1 mL of 1% SDS buffer then boiled for 10 min. The pellet fraction was centrifuged at 13,000 *g* for 10 min, and the soluble portion was saved for analysis. 25 µl of the tubulin and MT fraction was analyzed and quantified via Western blot using mAb DM1A on the infrared imaging system (Odyssey).

Statistical analysis

All data are presented as mean ± SEM. Comparison between groups was performed using a *t* test with significance defined as $P \leq 0.05$.

We would like to thank Dr. Kevin Sonnemann for generating the Dp260 baculovirus expression construct and Dr. Sonnemann and Thomas Cheever for their helpful discussions.

This work was supported by the National Institutes of Health Training Program in Muscle Research (AR007612), a grant from the National Institutes of Health (AR042423), and Gregory Marzolf Muscular Dystrophy Fellowships to J.L. Humston and K.W. Prins. K.W. Prins is a member of the Medical Scientist Training Program at the University of Minnesota. E. Ralston, V. Tate, and A. Mehta were supported by the National Institutes of Health Intramural Research Program.

Submitted: 11 May 2009
Accepted: 6 July 2009

References

Altman, A., M. Szyper-Kravitz, and Y. Shoenfeld. 2007. Colchicine-induced rhabdomyolysis. *Clin. Rheumatol.* 26:2197–2199.

Andra, K., H. Lassmann, R. Bittner, S. Shorny, R. Fassler, F. Propst, and G. Wiche. 1997. Targeted inactivation of plectin reveals essential function in maintaining the integrity of skin, muscle, and heart cytoarchitecture. *Genes Dev.* 11:3143–3156.

Ayalon, G., J.Q. Davis, P.B. Scotland, and V. Bennett. 2008. An ankyrin-based mechanism for functional organization of dystrophin and dystroglycan. *Cell.* 135:1189–1200.

Barton, E.R., L. Morris, A. Musaro, N. Rosenthal, and H.L. Sweeney. 2002. Muscle-specific expression of insulin-like growth factor I counters muscle decline in *mdx* mice. *J. Cell Biol.* 157:137–148.

Bhosle, R.C., D.E. Michele, K.P. Campbell, Z. Li, and R.M. Robson. 2006. Interactions of intermediate filament protein synemin with dystrophin and utrophin. *Biochem. Biophys. Res. Commun.* 346:768–777.

Boomershine, K.H. 2002. Colchicine-induced rhabdomyolysis. *Ann. Pharmacother.* 36:824–826.

Bulinski, J.C., and G.G. Gundersen. 1991. Stabilization of post-translational modification of microtubules during cellular morphogenesis. *Bioessays.* 13:285–293.

Caglar, K., Z. Odabasi, M. Safali, M. Yenicesu, and A. Vural. 2003. Colchicine-induced myopathy with myotonia in a patient with chronic renal failure. *Clin. Neurol. Neurosurg.* 105:274–276.

Fuchs, E., and I. Karakesisoglou. 2001. Bridging cytoskeletal intersections. *Genes Dev.* 15:1–14.

Gennerich, A., and R.D. Vale. 2009. Walking the walk: how kinesin and dynein coordinate their steps. *Curr. Opin. Cell Biol.* 21:59–67.

Gonzalez-Garay, M.L., and F. Cabral. 1995. Overexpression of an epitope-tagged beta-tubulin in Chinese hamster ovary cells causes an increase in endogenous alpha-tubulin synthesis. *Cell Motil. Cytoskeleton.* 31:259–272.

Gundersen, G.G., M.H. Kalnoski, and J.C. Bulinski. 1984. Distinct populations of microtubules: tyrosinated and nontyrosinated alpha tubulin are distributed differently in vivo. *Cell.* 38:779–789.

Gundersen, G.G., S. Khawaja, and J.C. Bulinski. 1987. Postpolymerization detyrosination of alpha-tubulin: a mechanism for subcellular differentiation of microtubules. *J. Cell Biol.* 105:251–264.

Guo, L., L. Degenstein, J. Dowling, Q.C. Yu, R. Wollmann, B. Perman, and E. Fuchs. 1995. Gene targeting of BPAG1: abnormalities in mechanical strength and cell migration in stratified epithelia and neurologic degeneration. *Cell.* 81:233–243.

Harada, A., K. Oguchi, S. Okabe, J. Kuno, S. Terada, T. Ohshima, R. Sato-Yoshitake, Y. Takei, T. Noda, and N. Hirokawa. 1994. Altered microtubule organization in small-calibre axons of mice lacking tau protein. *Nature.* 369:488–491.

Harper, S.Q., M.A. Hauser, C. DelloRusso, D. Duan, R.W. Crawford, S.F. Phelps, H.A. Harper, A.S. Robinson, J.F. Engelhardt, S.V. Brooks, and J.S. Chamberlain. 2002. Modular flexibility of dystrophin: implications for gene therapy of Duchenne muscular dystrophy. *Nat. Med.* 8:253–261.

Hirokawa, N., and Y. Noda. 2008. Intracellular transport and kinesin superfamily proteins, KIFs: structure, function, and dynamics. *Physiol. Rev.* 88:1089–1118.

Hoffman, E.P., R.H. Brown Jr., and L.M. Kunkel. 1987. Dystrophin: the protein product of the Duchenne muscular dystrophy locus. *Cell.* 51:919–928.

Hughes, J.R., A.M. Meireles, K.H. Fisher, A. Garcia, P.R. Antrobus, A. Wainman, N. Zitzmann, C. Deane, H. Ohkura, and J.G. Wakefield. 2008. A microtubule interactome: complexes with roles in cell cycle and mitosis. *PLoS Biol.* 6:e98.

Judge, L.M., M. Haraguchiln, and J.S. Chamberlain. 2006. Dissecting the signaling and mechanical functions of the dystrophin-glycoprotein complex. *J. Cell Sci.* 119:1537–1546.

Leung, C.L., K.J. Green, and R.K. Liem. 2002. Plakins: a family of versatile cytolinker proteins. *Trends Cell Biol.* 12:37–45.

Ohlendieck, K., and K.P. Campbell. 1991. Dystrophin-associated proteins are greatly reduced in skeletal muscle from mdx mice. *J. Cell Biol.* 115:1685–1694.

Ohlendieck, K., J.M. Ervasti, K. Matsumura, S.D. Kahl, C.J. Leveille, and K.P. Campbell. 1991. Dystrophin-related protein is localized to neuromuscular junctions of adult skeletal muscle. *Neuron.* 7:499–508.

Percival, J.M., P. Gregorevic, G.L. Odom, G.B. Banks, J.S. Chamberlain, and S.C. Froehner. 2007. rAAV6-microdystrophin rescues aberrant Golgi complex organization in mdx skeletal muscles. *Traffic.* 8:1424–1439.

Petrof, B.J., J.B. Shrager, H.H. Stedman, A.M. Kelly, and H.L. Sweeney. 1993. Dystrophin protects the sarcolemma from stresses developed during muscle contraction. *Proc. Natl. Acad. Sci. USA.* 90:3710–3714.

Prins, K.W., D.A. Lowe, and J.M. Ervasti. 2008. Skeletal muscle-specific ablation of gamma(cyto)-actin does not exacerbate the mdx phenotype. *PLoS ONE.* 3:e2419.

Ralston, E., Z. Lu, and T. Ploug. 1999. The organization of the Golgi complex and microtubules in skeletal muscle is fiber type-dependent. *J. Neurosci.* 19:10694–10705.

Rybakova, I.N., K.J. Amann, and J.M. Ervasti. 1996. A new model for the interaction of dystrophin with F-actin. *J. Cell Biol.* 135:661–672.

Rybakova, I.N., J.R. Patel, K.E. Davies, P.D. Yurchenco, and J.M. Ervasti. 2002. Utrophin binds laterally along actin filaments and can couple costameric actin with sarcolemma when overexpressed in dystrophin-deficient muscle. *Mol. Biol. Cell.* 13:1512–1521.

Rybakova, I.N., J.L. Humston, K.J. Sonnemann, and J.M. Ervasti. 2006. Dystrophin and utrophin bind actin through distinct modes of contact. *J. Biol. Chem.* 281:9996–10001.

Sonnemann, K.J., D.P. Fitzsimons, J.R. Patel, Y. Liu, M.F. Schneider, R.L. Moss, and J.M. Ervasti. 2006. Cytoplasmic gamma-actin is not required for skeletal muscle development but its absence leads to a progressive myopathy. *Dev. Cell.* 11:387–397.

Stone, M.R., A. O'Neill, D. Catino, and R.J. Bloch. 2005. Specific interaction of the actin-binding domain of dystrophin with intermediate filaments containing keratin 19. *Mol. Biol. Cell.* 16:4280–4293.

Stone, M.R., A. O'Neill, R.M. Lovering, J. Strong, W.G. Resneck, P.W. Reed, D.M. Toivola, J.A. Ursitti, M.B. Omary, and R.J. Bloch. 2007. Absence of keratin 19 in mice causes skeletal myopathy with mitochondrial and sarcolemmal reorganization. *J. Cell Sci.* 120:3999–4008.

Suzuki, A., M. Yoshida, H. Yamamoto, and E. Ozawa. 1992. Glycoprotein-binding site of dystrophin is confined to the cysteine-rich domain and the first half of the carboxy-terminal domain. *FEBS Lett.* 308:154–160.

Takahashi, M., H. Shiraishi, Y. Ishibashi, K.L. Blade, P.J. McDermott, D.R. Menick, D. Kuppuswamy, and G. Cooper IV. 2003. Phenotypic consequences of beta1-tubulin expression and MAP4 decoration of microtubules in adult cardiocytes. *Am. J. Physiol. Heart Circ. Physiol.* 285:H2072–H2083.

Warner, L.E., C. DelloRusso, R.W. Crawford, I.N. Rybakova, J.R. Patel, J.M. Ervasti, and J.S. Chamberlain. 2002. Expression of Dp260 in muscle tethers the actin cytoskeleton to the dystrophin-glycoprotein complex and partially prevents dystrophy. *Hum. Mol. Genet.* 11:1095–1105.

Way, M., B. Pope, R.A. Cross, J. Kendrick-Jones, and A.G. Weeds. 1992. Expression of the N-terminal domain of dystrophin in *E. coli* and demonstration of binding to F-actin. *FEBS Lett.* 301:243–245.

Wilbur, K., and M. Makowsky. 2004. Colchicine myotoxicity: case reports and literature review. *Pharmacotherapy.* 24:1784–1792.

Williams, M.W., and R.J. Bloch. 1999. Differential distribution of dystrophin and beta-spectrin at the sarcolemma of fast twitch skeletal muscle fibers. *J. Muscle Res. Cell Motil.* 20:383–393.